

Phonon dispersion in Sr₂RuO₄ studied by a first-principles cumulative force-constant approach

Y. Wang, J. J. Wang, J. E. Saal, S. L. Shang, L.-Q. Chen, and Z.-K. Liu

Materials Science and Engineering, The Pennsylvania State University, University Park, Pennsylvania 16802, USA

(Received 3 June 2010; revised manuscript received 29 September 2010; published 9 November 2010)

The phonon frequencies along several high symmetry lines for Sr₂RuO₄ were calculated using the real-space cumulative force-constant approach. Except for the highest Δ_1 ($\xi 00$) and Σ_3 ($\xi \xi 0$) dispersions, all other 54 branches were quantitatively described very well, including the anomalous softening of the RuO₆ octahedra rotational mode which was the lowest Σ_3 dispersion along the ($\xi \xi 0$) direction. We did not see any imaginary phonon modes for Sr₂RuO₄ and demonstrated that the softening of the rotational mode of the RuO₆ octahedra was not due to the anharmonic effects.

DOI: [10.1103/PhysRevB.82.172503](https://doi.org/10.1103/PhysRevB.82.172503)

PACS number(s): 74.25.Kc, 63.20.kd, 63.20.dk

The study of lattice dynamics for copper oxide high-temperature superconductors has been a focus of interest ever since their discovery in 1986,¹ attempting to understand the role of electron-phonon interactions² on their superconductivity.³⁻⁸ As pointed out by the recent review by Kresin and Wolf,² there has been growing evidence, mainly from various experimental studies, that electron-phonon interactions could play important role in high T_c superconductivity of the cuprates. However, accurate first-principles calculations of the phonon frequencies of their parent compound La₂CuO₄ have been stymied by the strong correlation among the d electrons, the symmetry breaking due to antiferromagnetic ordering, and the splitting between longitudinal optic and transverse optic phonon modes due to long range dipole-dipole interactions. The finding⁹ of superconductivity in Sr₂RuO₄, which possesses excellent metallic properties at low temperatures with tetragonal structure and for which no long range antiferromagnetic ordering is observed¹⁰ up to as low as 1.5 K, makes it feasible a complete first-principles calculation of phonon properties for compounds with crystal structure similar to the high-temperature tetragonal La₂CuO₄ phase.

In this work, we report the calculated phonon frequencies for Sr₂RuO₄ using the real-space cumulative force-constant approach,¹¹⁻¹⁴ which will be briefed below in Eqs. (1) and (2). The effects of supercell size and k -mesh settings on the calculated phonon dispersions are also examined. The first-principles static calculation of Sr₂RuO₄ at 0 K was performed with the projector-augmented wave method^{15,16} implemented in the Vienna *ab initio* simulation package (VASP, version 5.2). The exchange-correlation functional of the generalized gradient approximation (GGA) according to Perdew-Burke-Ernzerhof¹⁷ was employed in all calculations. For the static calculations of the seven-atom primitive unit cell, we used a Γ -centered $11 \times 11 \times 11$ k -mesh together with an energy cutoff of 500 eV.

In principle, anharmonic effects¹⁸ can be accounted for within the finite difference approach to lattice dynamics, in which the force constants between the atoms are calculated by moving an atom by a small displacement from its equilibrium position. In comparison, density-functional-perturbation theory¹⁹ for lattice dynamics assumes that the electrons linearly response to the change in lattice geometry without actually moving an atom. For this reason, the information of anharmonic effects might be lost in the calculated

force constants by density-functional-perturbation theory. Accordingly, both the finite difference approach and the density-functional-perturbation theory as implemented in VASP 5.2 are adopted in calculating the real-space cumulative force constants in this work. These are performed with an energy cutoff of 500 eV as well as with various k meshes and supercell sizes to examine the parameter effects on the calculated phonon frequencies.

The phonon frequencies were obtained¹⁴ by the solving the dynamic matrix of

$$\tilde{D}_{\alpha\beta}^{jk}(\mathbf{q}) = \frac{1}{\sqrt{\mu_j \mu_k}} \sum_P^N \phi_{\alpha\beta}^{jk}(0, P) \exp\{i\mathbf{q} \cdot \mathbf{R}(P)\}, \quad (1)$$

where $\phi_{\alpha\beta}^{jk}$ is the cumulative force constants the between atom j in the primitive cell M and atom k in the primitive cell P calculated using the conventional supercell method, \mathbf{q} the wave vector, α and β the Cartesian axes, N the number of primitive unit cells in the supercell, μ_j is the atomic mass of the j th atom in the primitive unit cell, and $\mathbf{R}(P)$ the position of the P th primitive unit cell in the supercell.

In using the finite difference approach or supercell approach, inaccuracies are thought to arise from the truncation of the force constants.^{19,20} This is not completely true as demonstrated by our recent works for the calculations of phonon properties for polar materials¹⁴ of α -Al₂O₃, MgO, c -SiC, and h -BN, and the calculations of the phonon dispersions for Mott-Hubbard insulators¹³ of NiO and MnO. At this point, we want to clarify some important aspects of the cumulative force-constant approach. Since we employ the supercell method, the calculated $\phi_{\alpha\beta}^{jk}$ is, in fact, the cumulative contributions of the atom indexed by k and P in the supercell and all its images by translational transformation of the supercell in the whole space. Let \mathbf{L}_i ($i=1, 2$, and 3) represent the lattice vectors of the supercell, then

$$\phi_{\alpha\beta}^{jk}(0, P) = \sum_{n_1=-\infty, n_2=-\infty, n_3=-\infty}^{\infty} \varphi_{\alpha\beta}^{jk}(0, P + n_1 \mathbf{L}_1 + n_2 \mathbf{L}_2 + n_3 \mathbf{L}_3), \quad (2)$$

where $\varphi_{\alpha\beta}^{jk}$ represents the true two-atom interaction force constant only between the atom j in the referenced supercell and atom k in the supercell positioned at $P + n_1 \mathbf{L}_1 + n_2 \mathbf{L}_2 + n_3 \mathbf{L}_3$. Since the exact wave vectors \mathbf{q}_{exact} satisfies

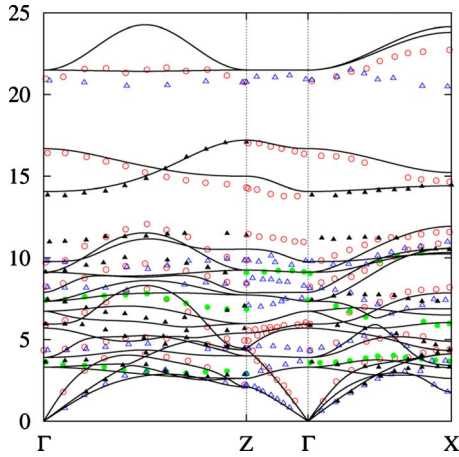


FIG. 1. (Color online) Calculated phonon dispersions (solid curves) of Sr_2RuO_4 using a $2a \times 2a \times 2c$ supercell and the finite difference approach. The symbols are the measured data by Braden *et al.* (Ref. 22) with, from left to right, \circ : Δ_1 , \bullet : Δ_2 , \triangle : Δ_3 , and \blacktriangle : Δ_4 representing Γ -Z ($\xi 00$) dispersions; \circ : Λ_1 , \bullet : Λ_2 , and \triangle : Λ_3 for Z- Γ (00ξ) dispersions; and \circ : Σ_1 , \bullet : Σ_2 , \triangle : Σ_3 , and \blacktriangle : Σ_4 for Γ -X ($\xi\xi 0$) dispersions.

$\mathbf{q}_{\text{exact}} \cdot \mathbf{L} = 2\pi k_l$, where k_l is an integer,^{19,21} one immediately learns that by Eq. (1)

$$\tilde{D}_{\alpha\beta}^{jk}(\mathbf{q}_{\text{exact}}) = \frac{1}{\sqrt{\mu_j \mu_k}} \sum_{X=-\infty}^{\infty} \varphi_{\alpha\beta}^{jk}(0, X) \exp\{i\mathbf{q}_{\text{exact}} \cdot \mathbf{R}(X)\}. \quad (3)$$

Note in Eq. (3) the summation over the index X now runs over all the primitive cells in the whole space indicated by the infinite summation range whereas in Eq. (1) the summation over the index P only runs over the number of primitive unit cells in the supercell. Therefore, the phonon frequencies calculated at the exact wave vectors by the cumulative force-constant approach are exact and the supercell size will not lead to errors in the calculated phonon frequencies.²¹ Generally speaking, if a supercell contains N primitive unit cells, one can always find N corresponding exact wave vectors in the \mathbf{q} space. In most linear response calculations, the common choice of a $4 \times 4 \times 4$ \mathbf{q} mesh is exactly correspondent to the $4 \times 4 \times 4$ supercell in the real space.

In Fig. 1, we show the calculated phonon dispersions for Sr_2RuO_4 using the 112-atom $2a \times 2a \times 2c$ supercell, $4 \times 4 \times 4$ Monkhorst k -mesh and the finite difference approach at the experimental equilibrium geometry reported by Maeno *et al.*⁹ of $a = 3.87$ Å and $c = 12.74$ Å (the internal atomic positions have been theoretically optimized) together with the recently measured phonon frequencies from inelastic neutron scattering by Braden *et al.*²² In general, the measured data are predicted rather well by the present work, except for the highest Δ_1 dispersion along the Γ -Z ($\xi 00$) direction and the Σ_3 dispersion (the second highest curve) along the Γ -X ($\xi\xi 0$) direction.

For the highest Δ_1 ($\xi 00$) dispersion, our calculations predict a rather high bump in the middle of this branch, marking the largest disagreement between the present calculation and

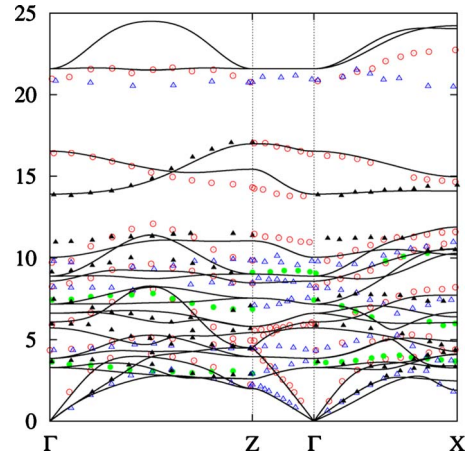


FIG. 2. (Color online) Calculated phonon dispersions (solid curves) of Sr_2RuO_4 using a $2\sqrt{2}a \times 2\sqrt{2}a \times c$ supercell and the finite difference approach. The symbols are the measured data by Braden *et al.* (Ref. 22) with the same meaning as Fig. 1.

the experiment by Braden *et al.*²² The second disagreement between the present calculation and the experiment by Braden *et al.*²² is shown by the highest Σ_3 ($\xi\xi 0$) dispersion as assigned by Braden *et al.*²² These two dispersions are very interesting. For $\text{La}_{1.9}\text{Sr}_{0.1}\text{CuO}_4$, the corresponding experimental Δ_1 ($\xi 00$) dispersion shows a rather deep dip in the middle and the Σ_3 ($\xi\xi 0$) dispersion shows very steep downward behavior.

To find out if the above-mentioned disagreements between the present calculation and the experiment²² is due to the effect of the adopted supercell shape by the present calculation, we performed a calculation using the 112-atom $2\sqrt{2}a \times 2\sqrt{2}a \times c$ supercell, $2 \times 2 \times 2$ Γ -centered k mesh, and the finite difference approach at the experimental equilibrium geometry. The results are shown in Fig. 2. What we find is that the disagreement between the calculation and the experiment remains the same.

The lowest Σ_3 ($\xi\xi 0$) dispersion possesses a rather soft frequency, as seen in the dip when approaching to the X point (0.5, 0.5, 0), due to the rotational mode of the RuO_6 octahedron around the c axis.^{22,23} Braden *et al.* (note that the X point labeled in this work was labeled as M point in Ref. 22) have suggested this soft mode is related to the structural phase transition observed in $\text{Ca}_{2-x}\text{Sr}_x\text{RuO}_4$, due to the close connection between the static octahedron rotation and the electronic and magnetic properties. Braden *et al.*²² also tried to attribute the behavior of the rotational mode to electron-phonon interactions. At first glance, the theoretical success for the current prediction of the lowest phonon branch along the Γ -X direction appears due to the use of the finite difference method. However, this is not the case, as shown by a calculation plotted in Fig. 3 using the 112-atom $2\sqrt{2}a \times 2\sqrt{2}a \times c$ supercell, $4 \times 4 \times 4$ Monkhorst k mesh, and density-functional-perturbation theory²⁴ at the experimental equilibrium geometry. Comparing Figs. 2 and 3, one finds the theoretical phonon frequencies predicted by the finite difference approach and the density-functional-perturbation theory are rather similar. Considering the difference in supercell shape, k mesh, and methods in calculating the force con-

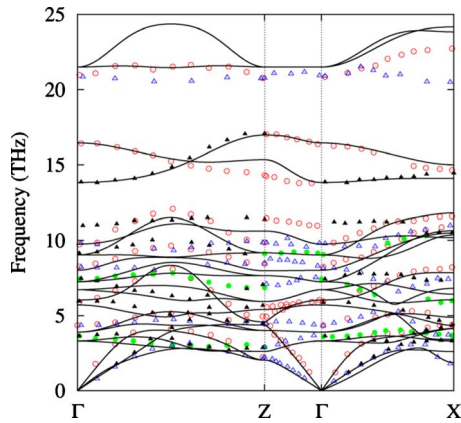


FIG. 3. (Color online) Calculated phonon dispersions (solid curves) of Sr_2RuO_4 using a $2\sqrt{2}a \times 2\sqrt{2}a \times c$ supercell and the linear response approach. The symbols are the measured data by Braden *et al.* (Ref. 22) with the same meaning as Fig. 1.

stants, we demonstrate that the softening of the rotational mode is not due to anharmonic effects.

For the above mentioned Σ_3 ($\xi\xi 0$) soft phonon mode, we see no anomaly or imaginary phonon frequencies along the Γ -X direction from the present calculation. Even the downward behavior of the rotational mode observed in the experiment is well predicted. This is in contrast to the *ab initio* tight-binding rigid ion model calculation made by Bauer and Falter²³ who predict a rather steep imaginary phonon dispersion for the above-mentioned rotational mode near the X point.

In the present calculation, the largest disagreement with experiments are found in the highest Δ_1 dispersion [half-breathing mode at $\mathbf{q}=(0.5,0,0)$] and the highest Σ_3 dispersion, showing that the electron-phonon effects are not properly included in the standard density-functional theory. The half-breathing mode anomaly is common in high-temperature superconductors. For the insulating state, when calculated using the local density approximation (or GGA),

the energy of this mode is much lower than the experimental value and it can be improved by using the LDA+ U method [e.g., Zhang *et al.*,²⁵]. In general, the role of U (Ref. 26) is to enhance the on-site force constant for Cu or Ru. For metallic Sr_2RuO_4 , Bauer and Falter²³ demonstrated that the frequencies of these modes increase with U , which improves the agreement with the experiment. In the present work, however, the energy of the half-breathing mode is already higher than experiment, so inclusion of U might probably not improve the result.

In summary, the phonon frequencies for the time-reversal symmetry breaking superconductor Sr_2RuO_4 have been calculated using the real-space cumulative force-constant approach and the overall agreement with experiment is excellent, except for the highest Δ_1 ($\xi 00$) and Σ_3 ($\xi\xi 0$) dispersions. We find that the softening of the rotational mode of the RuO_6 octahedra is not due to the anharmonic effects, as the calculated results are the same among the finite difference approach and density-functional-perturbation theory, together with the difference in supercell shape and k mesh in calculating the force constants.

This work was funded by the Office of Naval Research (ONR) under Contract No. N0014-07-1-0638, the National Science Foundation (NSF) under Grant No. DMR-1006557, and DOE Basic Sciences under Grant No. DOE DE-FG02-07ER46417 (Y.W. and L.Q.-C.), and in part supported by instrumentation funded by the National Science Foundation under Grant No. OCI-0821527. Calculations were also conducted at the LION clusters at the Pennsylvania State University and at the National Energy Research Scientific Computing Center, which is supported by the Office of Science of the U.S. Department of Energy under Contract No. DE-AC02-05CH11231. This work was also supported in part by a grant of HPC resources from the Arctic Region Supercomputing Center at the University of Alaska Fairbanks as part of the Department of Defense High Performance Computing Modernization Program.

¹J. G. Bednorz and K. A. Müller, *Z. Phys. B: Condens. Matter* **64**, 189 (1986).

²V. Z. Kresin and S. A. Wolf, *Rev. Mod. Phys.* **81**, 481 (2009).

³C. Falter and G. A. Hoffmann, *Phys. Rev. B* **64**, 054516 (2001).

⁴A. Lanzara, P. V. Bogdanov, X. J. Zhou, S. A. Kellar, D. L. Feng, E. D. Lu, T. Yoshida, H. Eisaki, A. Fujimori, K. Kishio, J. I. Shimoyama, T. Noda, S. Uchida, Z. Hussain, and Z. X. Shen, *Nature (London)* **412**, 510 (2001).

⁵K. P. Bohnen, R. Heid, and M. Krauss, *Europhys. Lett.* **64**, 104 (2003).

⁶T. P. Devereaux, T. Cuk, Z. X. Shen, and N. Nagaosa, *Phys. Rev. Lett.* **93**, 117004 (2004).

⁷L. Pintschovius, *Phys. Status Solidi B* **242**, 30 (2005).

⁸D. Reznik, L. Pintschovius, M. Ito, S. Iikubo, M. Sato, H. Goka, M. Fujita, K. Yamada, G. D. Gu, and J. M. Tranquada, *Nature (London)* **440**, 1170 (2006).

⁹Y. Maeno, H. Hashimoto, K. Yoshida, S. Nishizaki, T. Fujita, J.

G. Bednorz, and F. Lichtenberg, *Nature (London)* **372**, 532 (1994).

¹⁰J. L. Martinez, C. Prieto, J. Rodriguezcarvajal, A. Deandres, M. Valletregi, and J. M. Gonzalezcalbet, *J. Magn. Magn. Mater.* **140-144**, 179 (1995).

¹¹D. Alfè, *Comput. Phys. Commun.* **180**, 2622 (2009).

¹²K. Parliński, Z. Q. Li, and Y. Kawazoe, *Phys. Rev. Lett.* **78**, 4063 (1997).

¹³Y. Wang, J. E. Saal, J. J. Wang, A. Saengdeejing, S. L. Shang, L. Q. Chen, and Z. K. Liu, *Phys. Rev. B* **82**, 081104 (2010).

¹⁴Y. Wang, J. J. Wang, W. Y. Wang, Z. G. Mei, S. L. Shang, L. Q. Chen, Z. K. Liu, *J. Phys.: Condens. Matter* **22**, 202201 (2010).

¹⁵P. E. Blöchl, *Phys. Rev. B* **50**, 17953 (1994).

¹⁶G. Kresse and D. Joubert, *Phys. Rev. B* **59**, 1758 (1999).

¹⁷J. P. Perdew, K. Burke, and M. Ernzerhof, *Phys. Rev. Lett.* **77**, 3865 (1996).

¹⁸V. Merregalli and S. Y. Savrasov, *Phys. Rev. B* **57**, 14453 (1998).

- ¹⁹S. Baroni, S. de Gironcoli, A. Dal Corso, and P. Giannozzi, *Rev. Mod. Phys.* **73**, 515 (2001).
- ²⁰A. van de Walle and G. Ceder, *Rev. Mod. Phys.* **74**, 11 (2002).
- ²¹G. Kern, G. Kresse, and J. Hafner, *Phys. Rev. B* **59**, 8551 (1999).
- ²²M. Braden, W. Reichardt, Y. Sidis, Z. Mao, and Y. Maeno, *Phys. Rev. B* **76**, 014505 (2007).
- ²³T. Bauer and C. Falter, *J. Phys.: Condens. Matter* **21**, 395701 (2009).
- ²⁴M. Gajdoš, K. Hummer, G. Kresse, J. Furthmuller, and F. Bechstedt, *Phys. Rev. B* **73**, 045112 (2006).
- ²⁵P. Zhang, S. G. Louie, and M. L. Cohen, *Phys. Rev. Lett.* **98**, 067005 (2007).
- ²⁶U. D. Wdowik and D. Legut, *J. Phys.: Condens. Matter* **21**, 275402 (2009).